# Allophanes, a significant soil pool of silicon for plants

Sophie S. Cornu, Jean-Dominique Meunier, Céline Ratié, Fréderic Ouedraogo, Yves Lucas, Patricia Merdy, Doris Barboni, Camille Delvigne, Daniel Borschneck, Olivier Grauby, et al.

**Allophanes, a significant soil pool of silicon for plants**

Sophie Cornu (1), Jean-Dominique Meunier (1), Céline Ratie (2), Fréderic Ouedraogo (1), Yves Lucas (3), Patricia Merdy (3), Doris Barboni (1), Camille Delvigne (1, †), Daniel Borschneck (1), Olivier Grauby (4), Catherine Keller (1)

(1) Aix-Marseille Univ, CNRS, IRD, INRAE, Coll France, CEREGE, 13545 Aix en Provence, Cedex 4, France

(2) INRAE, InfoSol, 45075, Orléans, France.

(3) Université de Toulon, Aix-Marseille Univ., CNRS, IM2NP, 83041 Toulon Cedex 9, France

(4) Aix-Marseille Univ., CNRS – UMR 7325 CINaM, campus de Luminy, Case 913, 13288 Marseille Cedex 9, France

Corresponding author: Sophie Cornu (sophie.cornu@inrae.fr)

† present address: Earth and Life Institute, Environmental sciences, Université catholique de Louvain, L7.05.10, 1348, Louvain-la-Neuve, Belgium

**Abstract**

While in tropical soils recycling of plant phytoliths has been shown to represent a major pool of Si available for plants, the main Si pools available for plants in temperate soils are still poorly constrained. We characterised the various Si pools of temperate forested and cultivated soils in France by selecting seven paired sites (adjacent wheat and forest plots) for four soil groups: Luvisols, Albeluvisols, calcaric and hypereutric Cambisols. We showed that $CaCl_2$-extracted Si (bioavailable) is mostly controlled by pH and allophanes (short-range ordered aluminosilicates) but not by phytoliths. Cultivation, by decreasing the soil organic carbon content increases the allophane content and the $Si_{CaCl2}$ concentration. Our work highlights the importance of allophanes as the missing link between the soil solution and the clay minerals that could explain the reported correlation between the clay mineral content and bioavailable Si.

**Key words:** land use change, clay, phytolith, temperate ecosystems, bioavailable Si, pedogenesis

## 1- Introduction

The variability of Si content in soils is large, from less than 1 % wt in Histosols to greater than 45 % wt in some Podzols (Sommer et al., 2006). Si is included in a large number of soil solid phases of various origins: (1) minerals derived from the parent material as quartz, feldspar, phyllosilicates (e.g. muscovite, biotite) etc.; (2) solid phases resulting from the transformation by weathering and pedogenesis of the primary minerals into clay minerals (kaolinite, smectite, illite among others), crystalline and amorphous material, including poorly crystalline Fe oxides and short-range ordered (SRO) aluminosilicates (e.g. allophanes and imogolites); (3) amorphous silica particles (BSi) formed by Si biocycling and synthesized by plants (phytoliths), animals (sponge spicules) or protists (testate amoeba shells, diatom frustules) (Sommer et al., 2006; Puppe et al., 2015). While soils offer a wide range of Si sources, plants absorb Si only from the soil solution as $Si(OH)_4$. Therefore, deciphering the source of soluble Si (DSi) is challenging because of the complex biogeochemical interactions involving Si in soils (Schaller et al., 2021). The conversion of forest to cropland was shown to lead to several Si pool changes: (1) a decrease in the phytolith pool (Conley et al., 2008; Struyf et al., 2010; Guntzer et al., 2012; Vandevenne et al., 2015), in the easily soluble Si pool (Clymans et al., 2011) and the weathering of silicate minerals (Struyf et al., 2010) and (2) an increase in the pedogenic Si fraction i.e. clays (Vandevenne et al., 2015). In addition, the growing crops such as rice, sugar cane, or wheat (Hodson et al., 2005; Guntzer et al., 2012; Katz, 2015) that are among the most important Si accumulators (1% or more Si by dry weight) are predicted to change the global Si biogeochemistry in the future by increasing the reservoir of BSi on earth (Carey and Fulweiler, 2016)

Various methods have been used to estimate DSi and bioavailable Si (Liang et al., 2015). Their results suggest that bioavailable Si concentration is both negatively correlated with total Si content, reflecting the predominance of low solubility minerals such as quartz in the soils

(Yanai et al., 2016; Landré et al., 2020) and positively correlated with soil properties such as weatherable aluminosilicates (Li et al., 2020a), phytolith content (Li et al., 2020b; de Tombeur et al., 2020), pH (Klotzbücher et al., 2018; Meunier et al., 2018; Miles et al., 2014; Caubet et al., 2020), soil organic matter, iron oxides (Yanai et al., 2016) and the clay (< 2 µm) fraction contents (Liang et al., 2015; Yanai et al., 2016; Caubet et al., 2020).

In temperate soils, despite the observed decrease of soil phytolith content under agriculture, higher DSi (estimated by the $CaCl_2$ method referred to herein as $Si_{CaCl2}$) concentration was observed under agriculture compared to forest developed on sedimentary rocks (Vandevenne et al., 2015; Caubet et al., 2020). This was related to a higher pH observed in agricultural soils compared to forest soils (Caubet et al., 2020) pointing out two mechanisms: greater phytoliths dissolution, or greater adsorption onto clay minerals at higher pH. Cornu et al. (2012) also observed that the liming of agricultural soils in Europe induced a change in the nature of the clay minerals, and hence, potentially in the relative proportion of the different Si pools. Consequently, despite their lower solubility compared to phytoliths (Fraysse et al., 2009), clays may play an important role in maintaining high values of $Si_{CaCl2}$, somehow cancelling out the phytolith pool decrease (Vandevenne et al., 2015; Caubet et al., 2020).

To identify the mechanisms controlling $Si_{CaCl2}$ in temperate soils and to understand the impact of land use on these mechanisms in different soil types, we designed a paired-site approach in which we sampled adjacent soils differing only in their land use while other pedological factors (topography, parent material, climate, and age) were the same. Seven paired sites were selected with calcaric and non-calcaric soils, developed on sedimentary parent materials (limestone and loess). Beside the $Si_{CaCl2}$ pool, we measured the pools of Si associated to crystalline and amorphous material, including poorly crystalline Fe oxides and SRO-aluminosilicates, and biogenic Si particles. Only the topsoil horizons (0-0.3 m) were analysed as they were considered the most impacted by land use change.

## 2- Material and methods

### 2.1- Identification of the paired sites and sampling strategy

Paired sites are not easy to locate as they have to differ only by their land use, all other pedological factors (parent material, climate, topography, and time) being kept constant between the two sites (Filippi et al., 2016). We chose soils on sedimentary materials as land use impacts $Si_{CaCl2}$ on these soils, and calcaric and non-calcaric soils as their behaviour with respect to $Si_{CaCl2}$ differs (Caubet et al., 2020). In France, most cultivated soils with these characteristics are developed either on limestone or on decarbonised loess. We also chose to study soils with different degrees of pedogenetic evolution: calcaric and hypereutric Cambisols for limestone; Luvisols and Albeluvisol for loess (WRB, 2006). To identify the paired sites, we used the French Soil Quality Network (RMQS) of 2111 georeferenced sites in France spread over a regular grid (16*16 km) for which soil type, parent material and land use are provided (Jolivet et al., 2006).

All the RMQS sites with the appropriate parent material and soil type either cultivated or under forest, were extracted from the database. For each selected RMQS site, an adjacent site (i.e. with the same climate), with the same topographical position (therefore expected to be on the same type of soil and parent material) and under the complementary land use (either forest or cultivation) was identified on the basis of: (i) the maps of the French National Institute of Geographic and Forest Information (IGN, 1:25000); (ii) Cassini's maps, the oldest available maps with records of land use (Cassini, 1750), both available on Geoportail (https://www.geoportail.gouv.fr/); (iii) aerial photographs taken at different times during the 20$^{th}$ century. Only paired sites for which the land use change occurred more than 100 years ago were kept. In most cases, the forested areas have been preserved from cultivation because they belonged to the state or to castle parks. Nineteen pairs of adjacent plots were identified. Another paired site of Albeluvisol (WRB, 2006) on already well-characterised loess was

added (Montagne et al., 2016). The 20 sites were in the northern half of France (Table SI1), where the cultivation of wheat is common. Most of them included cereals in their rotation (Table SI1). Forests were mixed deciduous forests except for site 62 that had a conifer forest (Table SI1).

All the selected paired sites were auger-sampled and described in the spring of 2015. In the cultivated area, one sample was taken in the upper horizon which is homogenized by ploughing (usually 0-25 cm). In the nearby forested area two samples were taken (usually 0-5 and 5-25 cm). On the basis of the soil morphology, eighteen out of the 20 paired sites were kept and analysed for rare earth element (REE) concentrations and particle size distribution to detect potential changes in parent materials. Analyses were performed at the Laboratory of Soil Analysis (Arras, France). Seven paired sites were finally kept (Table SI1), as their REE and grain size skeleton patterns did not differ between land uses considering the analytical uncertainties (see supplementary information, SI, part 3 for more details) and thus could be considered as having the same parent material.

Bulk density measurements were performed using the volumetric cylinder method in cultivated areas and the excavation method in forested areas because the root density prevented the use of the cylinder. When bulk density could not be measured (e.g., at site 1166), it was estimated using the pedotransfer function proposed by Alexander (1980), which relates bulk density to soil organic carbon (SOC) content.

To compare the forested and cultivated sites, composite values (0-25 cm) were calculated for the forested sites considering the thickness of the two sampled horizons (0-5 cm and 5-25 cm) and their respective bulk densities.

### 2.2- Samples characterisation

### 2.2.1- Pedological analysis

Air dried samples were analysed for pedological characteristics at the Soil Analysis Laboratory of INRAE (Arras, France). The particle-size distribution was obtained by wet sieving and the pipette method (NF X 31-107). Total SOC concentration was measured by dry combustion (NF ISO 10694), CEC (cation exchange capacity) by the cobaltihexamine chlorine method (NF X 31-130), and pH in water with a 1:5 soil:water ratio (NF X 31-107).

The particle size fraction contents are hereafter denominated < 2 µm, 2-20 µm, 20-50 µm, 50-200 µm, 200-2000 µm.

The < 2 µm fraction CEC ($CEC_{<2µm}$) was calculated following equation 1.

$$CEC_{<2µm} = ((CEC - CEC_{SOC} * SOC) / < 2µm)*1000 \quad \text{(eq. 1)}$$

where SOC and <2 µm are the contents in SOC and in the <2 µm fraction, respectively. We used 200 $cmol^{+}\ kg^{-1}$ as an estimate of $CEC_{SOC}$ (Baize, 2000) of both the ploughed horizon of the cultivated site and for the 5-25 cm horizon of the forested plots and 100 $cmol^{+}\ kg^{-1}$ as an estimate of $CEC_{SOC}$ of the 0-5 cm horizon of the forested plots that contains a greater fraction of particulate organic matter with a lower CEC (Balesdent, pers. comm., 2018).

Total major elements concentrations in soil, including Si ($Si_{tot}$), were also analysed at the Soil Analysis Laboratory of INRAE (Arras, France) by ICP-MS analysis after HF tri-acid dissolution ($Al_{tot}$, $Fe_{tot}$, $Na_{tot}$, $Ca_{tot}$, $Mg_{tot}$, $K_{tot}$, $Mn_{tot}$) or alkaline fusion ($Si_{tot}$, NF ISO 14869-2).

### 2.2.2- Chemical extraction of different soil Si pools

We used three types of soft chemical extraction in parallel to access different soil Si pools:

(1) Soluble and bioavailable Si was extracted using the $CaCl_2$ method ($Si_{CaCl2}$; Haysom and Chapman, 1975; Narayanaswany and Prakash, 2010). The soils were mixed with a 0.01 mol $L^{-1}$ $CaCl_2$ solution with a solid/solution ratio of 10, in two replicates. The suspension was stirred for 16 h and filtered at 0.45 µm.

(2) Poorly crystalline Fe oxides and short-range ordered (SRO) aluminosilicates such as allophanes and imogolites were extracted by the oxalate method ($Si_o$, Tamm, 1922; Wada, 1989; Harsh, 2005). It is assumed that this method does not dissolve amorphous silica particles (i.e., phytoliths) (Kodama and Ross, 1991; Saccone et al., 2007). The $Si_o$ pool thus represents Si associated with amorphous co-precipitated Fe and Al compounds. Allophane content was estimated using Harsh's (2005) equation (2):

$$\% \text{ allophane} = Si_o/(- 0.067\ Al_o/Si_o + 0.27) \quad \text{(eq. 2)}$$

(3) Iron oxides were extracted by the dithionite-citrate-bicarbonate (DCB) method ($Si_d$, Mehra and Jackson, 1960), which also dissolves the poorly crystalline fraction and may dissolve phytoliths (Georgiadis et al., 2013).

Si extracted by these three methods and Fe and Al extracted by the latter two were measured using ICP-OES (Inductively Coupled Plasma Optical Emission Spectroscopy). Both $Si_o$ and $Si_d$ were extracted and measured at the Soil Analysis Laboratory of INRAE (Arras, France).

The different soil Si forms were then estimated considering that (i) the DSi equals the $Si_{CaCl2}$; (ii) Si in SRO minerals (allophanes, imogolites and poorly crystalline Fe oxides) equals ($Si_o$ - $Si_{CaCl2}$); (iii) Si associated to crystalline Fe oxides or to the part of phytoliths dissolved by the extractant equals ($Si_d$ - $Si_o$); and (iv) Si in crystalline silicates plus part of the phytoliths equals ($Si_{tot}$ - $Si_d$). We have to keep in mind that all these extractions are operationally defined

and may extract part of soil solid phases other than the targeted ones as already extensively discussed in the literature (e.g. Georgiadis et al., 2013).

Error bars were estimated considering 5 % uncertainty on the chemical and bulk density measurements.

### 2.2.3- Phytolith extraction and characterisation

Soil phytoliths were quantified, identified and their weathering state was evaluated.

BSi particles were extracted from the soils using wet digestion and heavy liquid separation (Jouquet et al., 2020; see SI part 2 for more details). No replicates have been done. Extracts, which happened to include phytoliths as well as low density particles such as micro-charcoals and amorphous silica skeletons of chrysophytes, diatoms, sponges, etc., were dried and weighed before being mounted on microscope slides to evaluate the real proportion of phytoliths versus non-phytolith particles in the extracts and, therefore, provide an estimation of the phytolith contents. We considered that phytoliths contained 42 % of Si (Alexandre et al., 1997) and could thus estimate the soil phytolith Si pool based on the phytolith abundances in the soils.

Since cultivated plants produce morphotypes of phytoliths different from forest species (trees, shrubs, ferns, forbs), phytolith taxonomic identification was performed according to the International Committee for Phytolith Taxonomy (2019) and counting was carried out.

Lastly, the analysis of the phytolith surface is a good indicator of their weathering state (Sommer et al., 2006; Jouquet et al., 2020), we measured the proportion of corroded vs non-corroded phytoliths (for more details, see SI part 2).

### 2.2.4- Mineralogical characterisation of the < 2 µm fraction

Dried soils were dispersed in 200 to 300 mL of ultrapure water by rotative shaking for 22 hours using plastic bottles and 20 agate balls (Ø 5 mm) (Balesdent et al., 1991). The mass of dried soil was chosen to obtain ca. 4 g of < 2 µm fraction. The suspension thus obtained was further dispersed by addition of 2 mL of Na-hexametaphosphate at 150 g $L^{-1}$, mechanical shaking, and 5-min ultrasonic dispersion. The < 2 µm fraction was then sampled according to the Stokes law and the settled soil particles resuspended for a new extraction step. The process was repeated until more than 80 % of the total fraction was recovered (that is more than 3.2 g of < 2 µm fraction out of 4 g). An aliquot of the < 2 µm suspension was dried to determine the < 2 µm suspension concentration. Oriented slides were made by deposition on glass slides of 10 mg of < 2 µm particles spiked with 10 % of boehmite added as a reference for X-ray diffraction (XRD) studies. The glass slides were then analysed with a Panalytical X'Pert Pro X-ray diffractometer equipped with a cobalt anti-cathode (λ = 1.79 Å) at 40 kV and 40 mA, with three treatments following Robert and Tessier (1974): air-dried (AD) and ethylene glycol (EG) solvation and heating at 490 °C for 4 hours.

Peak areas of the main mineral phases and boehmite were measured using the Fityk software (Wojdyr, 2010). The peak area ratio with respect to boehmite was used to compare samples.

Transmission electron microscope (TEM, JEOL JEM 2011) coupled to an energy-dispersive X-ray spectrometer (EDX, X-Flash Silicon Drift Detector 5030, Bruker) analysis was performed on the < 2µm fraction of sample BS3F1 (Table SI1) for checking the presence of allophanes.

## 2.3- Data analysis

Pedological characteristics and major element concentrations of the seven studied paired sites were analysed by principal component analysis (PCA). To identify different groups of soils from a pedological and chemical point of view, a hierarchical classification was performed on the first two factors of the PCA.

Soil characteristics of the paired sites were considered as different when the difference for a given soil characteristic exceeded the analytical uncertainties. As only one measurement by site was performed, no statistical tests could be performed to further test the statistical significance of this difference.

Significance of Pearson correlations between the $Si_{CaCl2}$ concentrations and different soil parameters was estimated based on the p-values considering a threshold level of 5 %.

All the statistical analyses were performed using the XLSTAT software for windows (Addinsoft).

## 3. Results

### 3.1. Seven paired sites with contrasted pedological characteristics and total concentrations of major elements

Pedological characteristics and total contents of major elements in the topsoils of the seven paired sites are reported in Tables SI1 and SI2. They were computed by PCA. The first two components explained 72 % of the dataset variance with 60% for the first component (Fig.1). The first component was correlated positively to $Ca_{tot}$, the < 2 µm fraction, $Fe_{tot}$, $Al_{tot}$, $Mg_{tot}$ and the SOC contents, as well to pH and the CEC, and negatively to $Si_{tot}$, $Na_{tot}$, silt (2-20 µm and 20-50 µm fractions) and fine sand (50-200 µm fraction) contents. The second component (12 % of the variance) was correlated positively to the 2-20 µm fraction, and negatively to the 50-200 µm fraction (Fig.1a). The PCA discriminated three groups of soils confirmed by a hierarchical clustering (Fig.1b). The first group corresponds to calcaric Cambisols and is positively correlated with the first PCA component, which means high pH, < 2 µm fraction, $Fe_{tot}$ and SOC contents. The second group corresponds to soils developed on loess (Luvisols and Albeluvisols) and is negatively correlated to the first PCA component, which means high 20-50 µm fraction and $Si_{tot}$ contents, low pH, $Fe_{tot}$ and SOC contents. The third group corresponds to hypereutric Cambisols and is intermediary between the other two groups, showing more similarities with the soils developed on loess than with the calcaric Cambisols.

Although the PCA did not highlight the impact of land use, pH and Si content in SRO were higher and SOC values lower under cultivation than under forest (Fig. 2). The CEC of the < 2 µm fraction did not differ with land use in Cambisols developed on limestone but was higher under cultivation in Luvisols and Albeluvisols developed on loess (Fig. 2).

### 3.2. Phytoliths of grasses were dominant in the two land uses

The relative abundances of the main phytolith types grouped according to plant types and confidence intervals are given in Table 1. On average, the biogenic silica extracts contained 89 % of phytoliths (range 51-99 %), the remaining fraction consisting of 3 % of other biogenic silica particles (range 0-8 %) and of 9 % charcoal (range 0-48 %); all particles had roughly the same size. For each soil, the mass of phytoliths corrected by phytolith relative abundance (in %) (Table 1) indicates that phytolith pools in soils ranged from < 0.01 to 0.616 g 100 $g^{-1}$ corresponding to 90 and up to 3978 kg Si $ha^{-1}$. For comparison, 800 kg Si $ha^{-1}$ was found in a rice field from Camargue, France (Desplanques et al., 2006), and values ranging from 450 to 1400 kg Si $ha^{-1}$ in French forest soils (Bartoli, 1983), using a similar procedure (heavy liquid extraction).

The phytolith contents were very low in calcaric Cambisols and Albeluvisols (Fig. 2i), for which there was no clear differences due to land use. For Luvisols, we observed clearly higher phytolith contents under forest (Fig. 2i). For the hypereutric Cambisols, a clear difference in the amount of phytoliths between land uses was also observed, although not always in the same direction: for the BS2 site more phytoliths were recorded under forest, while for the 1166 site more phytoliths were observed under cultivation (Fig. 2i).

Grass phytoliths (silica short cells and various silicified epidermal tissues) represented > 64 % in all forest and cultivated soil samples, except in forest samples 755-F1, 755-F2, and 1166-F1 (25 % only) (Fig. 3a). Phytoliths assigned to forest species (see Tables in SI part 2 for details) only represented 1-20 % of the total phytoliths sum, except in the forest soil sample 1166-F1 (45 %) (Fig. 3b). The proportions of ELONGATE DENDRITIC phytoliths, mainly produced by grass inflorescences, tended to be higher in the cultivated soils of the hypereutric Cambisols (Fig. 3c). Again, in the other soils their abundance was too low to discuss any differences between land uses (Fig. 3c). These results showed that in the forest soils, except for the forest site 1166, the forest-indicator phytoliths exhibited a very low abundance relative

to grass phytoliths (Fig 3), suggesting that wild grasses were the main producers of phytoliths in forest understorey.

The proportion of corroded phytoliths (ELONGATE and BLOCKY) was not different between forest and cultivated soils, except for samples from sites 1166 and BS2 where it was higher in the forest soil and in the cultivated soil respectively (Table 1).

### 3.3. Mineralogy of the < 2 µm fraction in the topsoils of the seven paired sites

The mineralogical composition of the < 2 µm fractions was rather similar for all forest soils (Fig. 4). All the fractions contained quartz (peak at 3.34 Å in all treatments), kaolinite (peak at 7.13 Å in both AD and EG treatments), illite (peak at 10 Å in all treatments), chlorite (peak at 14 Å in all treatments), poorly crystalline smectites and/or interlayered illite-smectite minerals (large bulgearound 12-11 Å for Na-exchanged samples shifting around 14 Å with glycol with no well-marked peak, more or less marked depending on the considered sample). Soils on loess clearly contained more quartz in their < 2 µm fraction than soils on limestone as shown by their higher quartz:boehmite peak ratio (Table SI3).

Cultivation appeared to slightly increase the amount of smectite and interlayered minerals and the amount of illite and decrease the amount of chlorite in soils on loess and in hypereutric Cambisols (Figs 4 b to d, and Table SI3). In calcaric Cambisols, however, cultivation seemed to result in a decrease of all clay minerals, possibly due to the non-dissolution of the carbonate fraction that acts as clay cement, with no clear change in proportion between the different types of clay minerals (Fig. 4a).

Transmission electron microscope (TEM) images showed the presence of discrete spherical particles with external diameter of 6 nm (Fig. 5). These spherical particles appear in the form of a disc with a white central part interpreted as being the projection of a hollow sphere.

### 3.4. Si pools in the topsoils of the seven paired sites assessed by chemical extractions

Whatever the soil type, more than 99% of $Si_{tot}$ was contained in crystalline silicates ($Si_{tot}$ - $Si_d$) (Fig. 2j). The other Si pools (Si in SRO minerals ($Si_o$ - $Si_{CaCl2}$), Si associated to crystalline oxides ($Si_d$ - $Si_o$) and Si in phytoliths) represented less than 0.3 % of the total soil Si. Si in SRO minerals was the most abundant of these pools in calcaric Cambisols, especially when cropped (Fig. 2g), while Si in phytoliths was the most abundant in Luvisols (Fig. 2i). Si associated to crystalline Fe oxides ($Si_d$ - $Si_o$) represented also a non-negligible part of the non-silicate Si pools, notably under forest (Fig. 2h). Part of this pool may originate from amorphous silica partly dissolved by the DCB reagent (Georgiadis et al., 2013). However, the pool associated to crystalline oxides ($Si_d$-$Si_o$) was clearly lower than the Si content in phytoliths, indicating that the phytoliths were not entirely dissolved by DCB.

The $Si_{CaCl2}$ pool represented a negligible proportion of the $Si_{tot}$ (Table 1) and was larger in soils developed on limestone than in soils developed on loess (Fig. 2f).

Cultivation increased both the $Si_{CaCl2}$ pool, especially in soils on loess, and the SRO-Si pool, especially in soils on limestone parent material (Fig. 2g). Cultivation, however, did not seem to modify the amount of Si associated to well-crystalline iron oxides and included in crystalline silicates (Fig. 2h and j).

## 4. Discussion

### 4.1 Allophanes are responsible for the $Si_{CaCl2}$ concentration in forest soils

When considering the 21 soil samples of the seven paired sites, the correlations between $Si_{CaCl2}$ and other soil parameters were in a good agreement with previous studies for the following parameters:

1) positive correlations between $Si_{CaCl2}$ and the < 2 μm fraction and its composition ($CEC_{<2\mu m}$, $Al_{tot}$, $Fe_{tot}$), pH, CEC (Table 2), as already observed by Caubet et al. (2020), but also between $Si_{CaCl2}$ and $Si_o$ and $Si_d$ (that contains $Si_o$ see section 2.2.2). Such positive correlations of $Si_{CaCl2}$ with $Si_o$ and $Si_d$ were already observed for many soil types by Yanai et al. (2016).

2) a negative correlation of $Si_{CaCl2}$ with $Si_{tot}$ (Table 2), which can be explained by the predominance of low solubility minerals such as quartz in the total Si pool (Yanai et al., 2016; Landré et al., 2020).

However, contrary to previous studies made for very different soils, $Si_{CaCl2}$ was not positively correlated with iron oxide (estimated by $Fe_d$) contents (a sandy soil with very low content of $Si_{CaCl2}$; de Tombeur et al., 2020) or the amount of phytoliths (estimated by $Na_2CO_3$ for Podzol and Chernozem, Li et al., 2020a) (Table 2). Li et al. (2020b) demonstrated that the extraction by $Na_2CO_3$ gave very different results from the extraction of phytoliths through heavy liquid separation. In the studied soils, the phytolith abundances estimated through heavy liquid separation were negatively correlated to the pH of forest soils (r= - 0.826, p-value = 0.022). This result agrees with an increasing solubility of phytoliths with increasing pH (Fraysse et al., 2009). As a result, the amount of phytoliths in the calcaric Cambisol and in the hypereutric Cambisol 1166, that had a pH value close to 7 (Table SI1), was low. It was also the case for the Albeluvisol despite a soil pH value of 5.2 (Table SI1). In this soil, reducing conditions occurring in winter and resulting in a transient high pH (Cornu et al., 2018) may be

responsible for an increase in the phytolith dissolution over that period. For the Luvisols and the BS2 hypereutric Cambisol, the amount of phytoliths in forest increased as the pH decreased. The absence of correlation between $Si_{CaCl2}$ and phytoliths suggests that this pool is however not the main pool controlling the $Si_{CaCl2}$ in temperate soils and that another pool of pedogenic origin must exist as already evoked by Vandevenne et al. (2015) and Keller et al. (2021).

$Si_o$ was very strongly correlated with $Al_o$ (Fig. 6a), excluding the cultivated calcaric Cambisol 701 that was very rich in SOC compared to the other cultivated soils (Fig. 2c and discussion below). Contrarily $Si_o$ was not significantly correlated with $Fe_o$ in cultivated plots ($r = 0.6$, p-value = 0.2) or in forests ($r = 0.5$, p-value = 0.3). In addition, the $Al_o/Si_o$ ratio observed for both forest and cultivated soils was close to 2, a typical value for allophanes (Harsh, 2005; Wada, 1989). Hence, it is likely that the $Si_o$ pool consisted in SRO aluminosilicates. SRO aluminosilicates are found in most soils, including those developed on loess and sedimentary rocks as in this study, insofar as their DSi are between 0.1 and 4 mmol $L^{-1}$ (Harsh, 2005). DSi values close to 0.1 mmol $L^{-1}$ were indeed obtained for the soil solution of the BS3 soil (Cornu et al., 2018). In addition, the spherical particles observed by TEM (Fig. 5) are commonly interpreted as allophanes (Kitagawa, 1971; Henmi and Wada, 1976; Parfitt, 1990).

Our dataset shows also a strong correlation between the < 2 µm fraction and the allophane contents (Fig. 6b), suggesting that allophanes may either be a product of clay mineral weathering or be part of the clay mineral formation, notably of the finest clays, the smectites and/or interlayered clay minerals that were shown to be present in all the soils considered (Fig. 4). Li et al. (2020a) also observed the formation of allophanes in a pot experiment as the result of weathering. When the $Al_o/Si_o$ ratio is above 2, which is the case in most forest soils (Table 1 and SI2), the $Al_o$ content in excess is present as Al-OC complexes (Harsh, 2005).

These Al-OC complexes partially preclude the formation of short range ordered aluminosilicates (Harsh, 2005).

$Si_{CaCl2}$ was well correlated to allophane content (Fig. 7a), excluding the BS2 site for which part of the $Si_o$ extracted was not contained in allophanes contrarily to all the other sites ( as calculated by eq. 2). Therefore, allophanes are assumed to control a fraction of $Si_{CaCl2}$ in soils. This agrees well with the high $Si_{CaCl2}$ content observed in Andosols, which contain a large amount of imogolites and allophanes (Caubet et al. 2020).

Caubet et al. (2020) concluded that $Si_{CaCl2}$ was controlled by both sorption and dissolution processes, which are strongly controlled by pH for soils with < 2 µm fractions both larger than 50 g $kg^{-1}$ and lower than 325 g $kg^{-1}$. For Indian soils this relation is not linear but polynomial, with a stabilisation of the $Si_{CaCl2}$ concentrations for pH higher than 7 (Meunier et al., 2018). We used a comparable relationship for the soils considered here excluding the BS2 and 62 forest soils (Fig. 7b).

The pH value of the 62 forest plot lower than 4.5 suggests the beginning of podzolisation (Caner et al., 2010; Sauer et al., 2008; Fekiacova et al., 2017). The conifer vegetation observed on this plot (Table SI1) is compatible with the onset of such a process. This low pH also corresponds to the upper limit of the Al/Fe oxide buffer range (Stützer, 1998). Podzolisation induces dissolution of the clay minerals, which may be responsible for the higher $Si_{CaCl2}$ concentration observed with respect to the regression model presented in Fig. 7b.

The above findings have the following consequences on the terrestrial Si cycle described by Struyf et al. (2010). In all soil types, 99 % of Si was contained in crystalline silicates. However, in soils developed on loess almost 60 % of the crystalline silicates consisted of quartz (e.g., Montagne et al., 2008 for BS3), a poorly weatherable mineral. In the calcaric

Cambisols, the total Si content in crystalline silicate was much lower than in soils developed on loess and was mainly contained in clay minerals and some quartz and feldspar. Despite this mineralogical difference, we concluded that the main weatherable mineral compartment contributing to $Si_{CaCl2}$ consists in the clay minerals (Fig. 8). This compartment was almost twofold larger in the calcaric Cambisols than in the soils on loess (Fig. 2a). The clay compartment controlled allophanes (Fig. 6b) which in turns controlled the $Si_{CaCl2}$ as discussed above. Allophanes are an easily available source of DSi as shown by dissolution rates much higher than those of phytoliths at pH lower than 9 (Ralston et al., 2021; Fraysse et al., 2009). Consequently, phytoliths did not appear to be the first source of $Si_{CaCl}$ in the considered soils, in agreement with Keller et al. (2021), who found that the clay minerals can compete with phytoliths as a main source of plant Si when the proportion of clay is high.

Reflecting the pH-dependent dissolution rate of phytoliths (Fraysse et al., 2009), the phytolith pool was lower in calcaric Cambisols (pH around 7, Table SI1) than in soils developed on loess (pH around 5, Table SI1). Consequently, the higher $Si_{CaCl2}$ in calcaric Cambisols compared to soils on loess could be explained by the higher amount of allophanes in calcaric Cambisol, but also, to a lesser extent, by a higher dissolution of the phytolith pool.

### 4.2. Impact of land use on the Si biogeochemical cycle and its various mineralogical pools

As expected, cultivation increased the soil pH (Fig. 2b) and decreased the SOC content (Fig. 2c) in all soils. For soils developed on loess, the pH was two units higher under cultivation than under forest because of liming. For calcaric Cambisols, the pH was one unit higher under cultivation than under forest because of the acidifying capacity of the forest (Fig. 2b, Table SI1).

We confirm here that cultivation increases the amount of $Si_{CaCl2}$ for soils developed on sediments (Caubet et al. 2020; Vandevenne et al. 2015; Klotzbücher et al., 2018). The change in pH and SOC induced by cultivation may act on the allophanes and phytoliths pools and therefore modify the terrestrial Si cycle.

Based on the literature, a lower phytolith content was expected in cultivated soils compared to topsoils under forest (Guntzer et al., 2012; Vandevenne et al., 2015). This was clearly observed for Luvisols, and to a lesser extent for the BS2 hypereutric Cambisol (Fig. 2i). This decrease in phytoliths may be explained by both a larger dissolution of phytoliths under cultivation due to the pH increase and phytolith exportation due to harvesting. The relative abundance of phytoliths (Fig. 3) suggests that wild grasses were the main producers of phytoliths in forest undergrowth. This is in agreement with temperate trees being poor Si accumulators (Bremond et al. 2004).

Cultivation had no clear impact on the phytolith pool in the calcaric Cambisol or in the Albeluvisols, where the amounts of extracted phytoliths were very low. The proportion of corroded phytoliths (ELONGATE and BLOCKY) was higher in the forest 1166 hypereutric Cambisol (Table 1), that also exhibits a lower amount of phytoliths than under cultivation. Differences in surface areas between grass and forest phytoliths might explain the observed proportions with a higher rate of dissolution of forest phytoliths (Wilding and Drees, 1974). However, this hypothesis is not supported by the laboratory measurements (Fraysse et al., 2009). Crop management through the restitution strategy of inedible plant parts and the crop rotation system may also lead to site fluctuation in exportation, maybe explaining the exception of the 1166 site. Indeed, crop straw recycling in agricultural soils have proven to be an efficient strategy for limiting desilication (Puppe et al., 2021).

By decreasing SOC (Fig. 2c), cultivation promotes the formation of allophanes that are twice as abundant under cultivation as under forest in the calcaric Cambisols and soils developed on

loess (Figs 2c and 5b). We observed $Al_o/Si_o$ ratios higher than 2 in forest but close to 2 in cultivated soils (Table 1), evidencing a decrease in the Al-OC complexes that prevent allophane formation under forest as discussed above. For the cultivated soils with a pH close to 8, pH may be less favourable to Si adsorption on allophanes that are at zero point of charges (Harsh, 2005). The high $Si_{CaCl2}$ values may then be explained by Si adsorbed on carbonate surfaces (Caubet et al. 2020).

Struyf et al. (2010) observe that cultivation decreases the exportation of DSi at the watershed outlet. They interpret this decrease in exportation by a reduction in the silicate mineral weathering. On the contrary, our results suggest that this decrease might be due to a higher retention of Si in the soils by the increase of allophane formation under cultivation (Fig. 8).

## 5- Conclusion

In temperate soils, phytoliths may not be the main Si pool contributing to bioavailable Si in contrast to tropical soils that are strongly depleted in Si and have kaolinite as dominant clay mineral. Temperate soils indeed exhibit a more complex clay mineral assemblage (smectite, illite, kaolinite and interlayered minerals). Allophanes - either precursors or dissolution products of these clay minerals - appear as the main Si pool contributing to DSi, estimated by $CaCl_2$ extraction. This explains the correlation between $Si_{CaCl2}$ and the clay fraction reported in the literature.

Cultivation seems to impact soil Si pools and DSi in two ways. First, cultivation increases pH by liming in the case of non-calcaric soils and by suppressing forest acidification. The increase in pH enhances Si sorption and phytolith dissolution. Secondly, cultivation decreases soil organic carbon, promoting the formation of allophanes. At pH lower than 4.5, other processes occur, such as podzolisation, modifying the relationship between DSi and pH.

So far, there has been a lot of emphasis put on phytoliths as a source of DSi. Our work highlights the importance of allophanes as the missing link between the soil solution and the clay minerals that could explain why clay minerals may be so important, despite lower solubility rates than phytoliths.

**Acknowledgments**

This work was performed in the framework of the French ANR BioSiSol project (ANR-14-CE01-0002). The authors are grateful to the CEES team (https://doi.org/10.15454/VCZ6BS) (INFOSOL, INRAE, Orléans) for their support in site selection, sampling and bulk density measurements and to B. Angeletti for ICP measurements at CEREGE.

**References**

Alexander, E. B. 1980. Bulk Densities of California Soils in Relation to Other Soil Properties. Soil Science Society of America Journal, 44, 689-692. doi:10.2136/sssaj1980.03615995004400040005x

Alexandre A., Meunier J.D., Colin F. and Koud J.M., 1997, Plant impact on the biogeochemical cycle of silicon and related weathering processes, Geochim. et Cosmochim. Acta, 61, 677-682.

Baize, D., 2000. Guide des analyses en pédologie, Quae. ed. INRA Editions, Paris (France).

Balesdent, J., Pétraud, J.P., Feller, C., 1991. Effet des ultrasons sur la distribution granulométrique des matières organiques des sols. Science du sol, 29 (2): 95-106.

Bartoli, F., 1983. The biogeochemical cycle of silicon in two temperate forest ecosystems. In: R. Hallberg (ed.) “Environmental Biogeochemistry”, Ecol. Bull., Stockholm, 35, 469-476.

Bremond, L., Alexandre, A., Vela, E., Guiot, J., 2004. Advantages and disadvantages of phytolith analysis for the reconstruction of Mediterranean vegetation: an assessment based on modern phytolith, pollen and botanical data (Luberon, France). Review of Palaeobotany and Palynology 129, 213–228. https://doi.org/10.1016/j.revpalbo.2004.02.002

Carey, J.C., Fulweiler, R.W., 2016. Human appropriation of biogenic silicon-the increasing role of agriculture. Functional Ecology 30, 1331-1339.

Cassini, C.F., 1750. Composite: Carte de France. Carte de France. Levee par ordre du Roy. Retrieved from. http://www.davidrumsey.com/xmaps10000.html.

Caner, L., Joussein, E., Salvador-Blanes, S., Hubert, F., Schlicht, J.-F., Duigou, N., 2010. Shorttime clay-mineral evolution in a soil chronosequence in Oléron Island (France). J. Plant Nutr. Soil Sci. 173, 591–600.

Caubet, M., Cornu, S., Saby, N.P.A., Meunier, J.D., 2020. Agriculture increases the bioavailability of silicon, a beneficial element for crop, in temperate soils. Sci Rep 10, 19999. https://doi.org/10.1038/s41598-020-77059-1

Conley, D.J., Likens, G.E., Buso, D.C., Saccone, L., Bailey, S.W., Johnson, C.E., 2008. Deforestation causes increased dissolved silicate losses in Hubbard Brook Experimental Forest. Global Change Biology 14, 1-7.

Cornu, S., Montagne, D., Hubert, F., Barré, P. and Caner, L., 2012. Evidence of short-term clay evolution in soils under human impact C. R. Geoscience 344: 747–757.

Cornu S.□, Samouëlian A.□, Ayzac A.□, Montagne D.□, 2018. Soluble and colloidal translocation of Al, Fe, Si and Mn in an artificially drained French Retisol. Geoderma, 330, 193-203. DOI: 10.1016/j.geoderma.2018.05.032

Clymans, W., Struyf, E., Govers, G., Vandevenne, F., Conley D.J., 2011. Anthropogenic impact on amorphous silica pools in temperate soils. Biogeosciences, 8, 2281–2293, 2011.25

Desplanques V., Cary L., Mouret J.C., Trolard F., Bourrié G., Grauby O., Meunier J.D., 2006. Silicon transfers in a rice field in Camargue (France). Journal of Geochemical Exploration, 88, 190-193.

de Tombeur, F., Turner, B.L., Laliberté, E., Lambers, H., Mahy, G., Faucon, M-P., Zemunik, G., Cornélis, J-T., 2020. Plants sustain the terrestrial silicon cycle during ecosystem retrogression. Science 369, 1245-1248.

Fekiacova Z., Vermeire M.L., Bechon L., Cornelis J.T., Cornu S., 2017. Can Fe isotope fractionations trace the pedogenetic mechanisms involved in podzolization? Geoderma 296: 38–46. https://doi.org/10.1016/j.geoderma.2017.02.020

Filippi P., Minasny B., Cattle S.R., Bishop T.F.A., 2016. Chapter Four - Monitoring and Modeling Soil Change: The Influence of Human Activity and Climatic Shifts on Aspects of Soil Spatiotemporally. In Advances in Agronomy, eds Sparks D.L., 139, 153-214, https://doi.org/10.1016/bs.agron.2016.06.001.

Fraysse F., Pokrovsky O.S., Schott J., Meunier J.D., 2009. Surface chemistry and reactivity of plant phytoliths in aqueous solutions. Chemical Geology, 258 (3–4): 197-206, https://doi.org/10.1016/j.chemgeo.2008.10.003.

Georgiadis, A., Sauer, D., Herrmann, L., Breuer, J., Zarei, M., Stahr, K., 2013. Development of a method for sequential Si extraction from soils. Geoderma, 209-210, 251-261.

Guntzer, F., Keller, C., Poulton, P.R., McGrath, S.P., Meunier, J.-D., 2012. Long-term removal of wheat straw decreases soil amorphous silica at Broadbalk, Rothamsted. Plant and Soil 352, 173–184.

Harsh J., 2005. Amorphous materials. In Encyclopedia of Soils in the Environment, Hillel D. eds, Elsevier, pp 64-71, https://doi.org/10.1016/B0-12-348530-4/00207-1.

Haysom, M.B.C., Chapman, L.S., 1975. Some aspects of the calcium silicate trials at Mackay. Proc. Qld. Soc. Sugar Cane Technol. 42, 117-122.

Henmi, T., Wada, K., 1976. Morphology and composition of allophane. Am. Mineral. 61, 379-90.

Hodson, M. J., White, P. J., Mead, A., Broadley, M. R., 2005. Phylogenetic variation in the silicon composition of plants. Annals of Botany 96, 1027–1046.

International Committee for Phytolith Taxonomy (ICPT), Neumann, K., Strömberg, C.A.E., Ball, T., Albert, R.M., Vrydaghs, L., Cummings, L.S., 2019. International Code for Phytolith Nomenclature (ICPN) 2.0. Annals of Botany. https://doi.org/10.1093/aob/mcz064

Jolivet, C., Boulonne, L., Ratié, C., 2006. Manuel du Réseau de Mesures de la Qualité des Sols.

Jouquet, P., Jamoteau, F., Majumdar, S., Podwojewski, P., Nagabovanalli, P., Caner, L., Barboni, D., Meunier, J.D., 2020. The distribution of silicon in soils influenced by termite bioturbation in South Indian forest soils. Geoderma. https://doi.org/10.1016/j.groderma.2020.114362.

Katz, O., 2015. Silica phytoliths in angiosperms: Phylogeny and early evolutionary history. New Phytol. 208, 642–646.

Keller, C., Rizwan, M., Meunier, J.D., 2021. Are clay minerals a significant source of Si for crops? A comparison of amorphous silica and the roles of the minerals type and pH. Silicon. https://doi.org/10.1007/s12633-020-00877-5

Kitagawa Y., 1971. The "unit particle" of allophane. Am. Mineral., 56, 465-475

Klotzbücher, T., Klotzbücher A., Kaiser K., Merbach I., Mikutta R., 2018. Impact of agriculture practices on plant-available silicon. Geoderma 331, 15-17.

Kodama, H., Ross, G.J. 1991. Tiron dissolution method used to remove and characterize inorganic components in soils. Soil Science Society of America Journal, 55, 1180–1187.

Landré, A., Cornu, S., Meunier, J.D., 2020. Do climate and land use affect the pool of total silicon concentration? A digital soil mapping approach of French topsoils. Geoderma 364, 114175.

Li, Z., Cornelis, J.T., Vander Linden, C., Van Ranst, E., Delvaux, B., 2020a. Neoformed aluminosilicates and phytogenic silica are competitive sinks in the silicon soil-plant cycle. Geoderma 114308.

Li, Z., de Tombeur, F., Vander Linden, C., Cornelis, J.T., Delvaux, B., 2020b. Soil microaggregates store phytoliths in a sandy loam. Geoderma, 360, doi.org/10.1016/j.geoderma.2019.114037

Liang, Y., Nikolic, M., Bélanger, R., Gong, H., Song, A., 2015. Silicon in Agriculture. (Springer Netherlands). doi:10.1007/978-94-017-9978-2.

Mehra, O. P. & Jackson, M. L., 1960. Iron Oxide Removal from Soils and Clays by a Dithionite-Citrate System Buffered with Sodium Bicarbonate. Clays and Clay Minerals 7, 317–327.

Meunier, J.-D., Sandhya, K., Prakash, N. B., Borschneck, D., Dussouillez, P., 2018. pH as a proxy for estimating plant-available Si? A case study in rice fields in Karnataka (South India). Plant and Soil 432, 143–155.

Miles, N., Manson, A. D., Rhodes, R., Antwerpen, R. van, Weigel, A., 2014. Extractable Silicon in Soils of the South African Sugar Industry and Relationships with Crop Uptake. Communications in Soil Science and Plant Analysis 45, 2949–2958.

Montagne D., Cousin, I., Cornu, S., 2016. Changes in the pathway and the intensity of albic material genesis: Role of agricultural practices. Geoderma, 268, 156–164

Montagne, D., Cornu, S., Le Forestier, L., Hardy, M., Josière, O., Caner, L. Cousin, I.. 2008. Impact of drainage on soil-forming mechanisms in a French Albeluvisol: input of mineralogical data in mass-balance modelling. Geoderma, 145, 426–438.

Narayanaswamy, C., Prakash, N.B., 2010. Evaluation of selected extractants for plant--Available Silicon in Rice Soils of Southern India. Communications in Soil Science and Plant Analysis, 41 (8), 977-989. https://doi.org/10.1080/00103621003646063

Parfitt R. L., 1990. Allophane in new Zeland - a review. Aust. J. Soil Res., 28, 343-60

Puppe, D., Ehrmann, O., Kaczorek, D., Wanner, M., Sommer, M., 2015. The protozoic Si pool in temperate forest ecosystems-quantification, abiotic controls and interactions with earthworms. Geoderma 243-244, 196-204.

Puppe, D., Kaczorek, D., Schaller, J., Barbusky, D., Sommer, M., 2021. Crop straw recycling prevents anthropogenic desilication of agricultural soil-plant systems in the temperate zone-Results from a long-term field experiment in NE Germany. Geoderma 403, 115187. https://doi.org/10.1016/j.geoderma.2021.115187

Ralston, S.J., Hausra, E.M., Tschauner, O., Rampe, E., Peretyazhko, T.E., Christoffersen, R., Defelice, C., Lee H., 2021. Dissolution rates of allophane with variable Fe contents: implications for aqueous alteration and the preservation of x-ray amorphous materials on Mars. Clays Clay Miner. 69, 263–288 (2021). https://doi.org/10.1007/s42860-021-00124-x

Robert, M., Tessier, D., 1974. Méthode de préparation des argiles des sols pour des études minéralogiques. Ann. Agron., 25, 859–882.

Saccone, L., Conley D.J., Koning, E., Sauer D., Sommer, M., Kaczorek, D., Blecker, S.W., Kelly, E.F., 2007. Assessing the extraction and quantification of amorphous silica in soils of forest and grassland ecosystems. Eur J Soil Sci, 58, 1446-1459.

Sauer, D., Schülli-Maurer, I., Sperstad, R., Soerensen, R., Stahr, K., 2008. Podzol development with time in sandy beach deposits in southern Norway. J. Plant Nutr., 171, 483–497.

Schaller, J., Puppe, D., Kaczorek, D., Ellerbrock, R., Sommer, M. 2021. Silicon Cycling in Soils Revisited. Plants 10, 295. https:// doi.org/10.3390/plants10020295

Sommer, M., Kaczorek, D., Kuzyakov, Y., Breuer, J., 2006. Silicon pools and fluxes in soils and landscapes—a review. J. Plant Nutr. Soil Sci., 169, 310–329. https://doi.org/10.1002/jpln.200521981

Struyf, E., Smis, A., Van Damme, S., Garnier, J., Govers, G., Van Wesemael, B., Conley, D.J., Batelaan, O., Frot, E., Clymans, W., 2010. Historical land use change has lowered terrestrial silica mobilization. Nat. Commun. 1, 129.

Stützer, A., 1998. Early stages of podzolisation in young aeolian sediments, western Jutland. Catena 32, 115–129.

Tamm, O., 1922. Eine Method zur Bestimmung der anorganishen Komponenten des Golkomplex in Boden. Medd. Statens skogforsoksanst. vol. 19 pp. 385–404.

Vandevenne, F., Struyf, E., Clymans, W., Meire, P., 2011. Agricultural silica harvest: have humans created a new loop in the global silica cycle? Front Ecol Environ 2012; 10 (5), 243–248, doi:10.1890/110046

Vandevenne, F.O., Barao, L., Ronchi, B., Govers, G., Meire, P., Kelly, E.F., Struyf., E., 2015. Silicon pools in human impacted soils of temperate zones. Global Biogeochemical Cycles, 29, doi:10.1002/2014GB005049.

WRB, 2006. World reference base for soil resources. World Soil Resources Reports, 103. FAO, Rome.

Wada, K., 1989. Allophane and imogolite, in: Minerals in Soil Environments, Dixon, J. B., Weed, S. B., & Wada, K. eds. Soil Science Society of America, Madison, USA, 1051–1087. doi:10.2136/sssabookser1.2ed.c21

Wilding, L.P., Drees, L.R., 1974. Contributions of Forest Opal and Associated Crystalline Phases to Fine Silt and Clay Fractions of Soils. Clays Clay Miner. 22, 295–306. https://doi.org/10.1346/CCMN.1974.0220311

Wojdyr, M., 2010, Fityk: a general-purpose peak fitting program, J. Appl. Cryst., 43, pp. 1126-1128.

Yanai, J., Taniguchi, H. & Nakao, A. Evaluation of available silicon content and its determining factors of agricultural soils in Japan. Soil Science and Plant Nutrition 62, 511–518 (2016).

## Figures

Figure 1: Principal component analysis (PCA) of the pedological characteristics and major element concentrations for the seven paired sites studied. a- Circle of correlations; b- space of the individuals (F states for forest and C for cultivation). Different symbols correspond to the different groups defined by a hierarchical classification performed on the first two factors of the PCA. Green diamonds encompass the calcaric Cambisols, blue circles the hypereutric Cambisols and red triangles correspond to soils developed on loess parent materials. Forest sites correspond to composite values (0-25 cm) calculated considering the thickness of the two sampled horizons (0-5 cm and 5-25 cm), their concentrations in the different elements and their respective bulk densities.

a

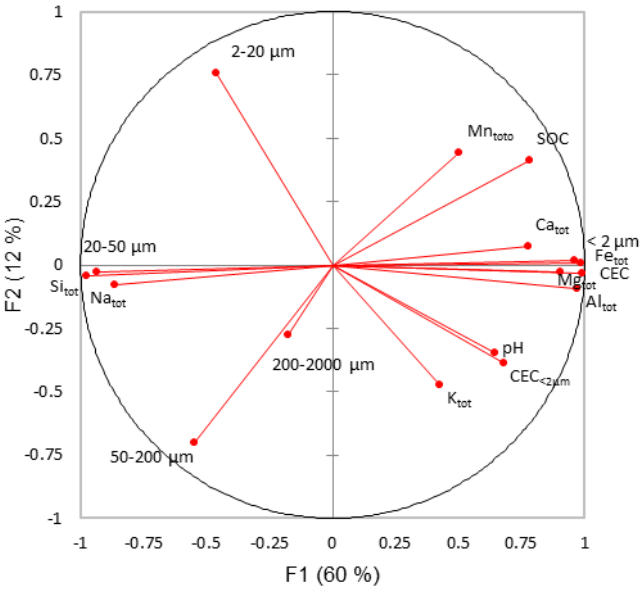


b

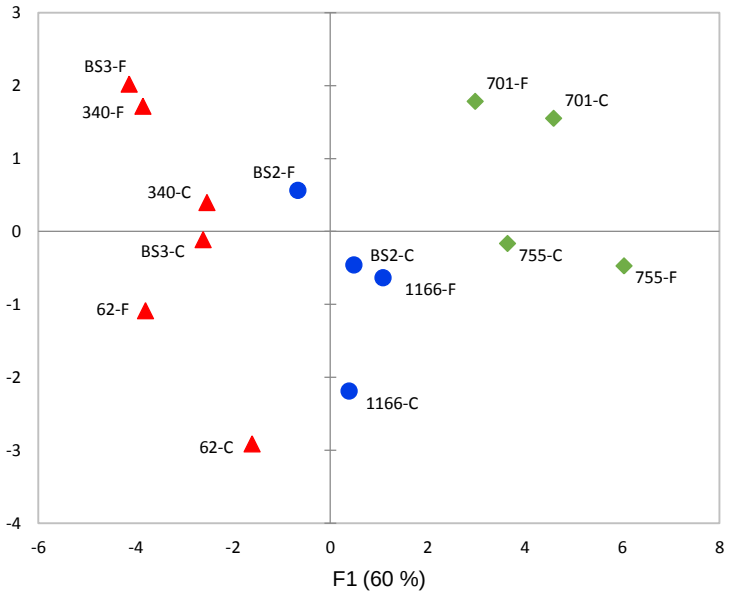

Fig 2: < 2 µm fraction (a), pH (b), SOC (c), CEC of the < 2 µm fraction (d) and the Fe in iron oxides ($Fe_d$; e), and different Si forms (f: soluble and bioavailable Si ($Si_{CaCl2}$); g: Si in SRO minerals ($Si_o$ - $Si_{CaCl2}$); h: Si in crystalline Fe oxides ($Si_d$ - $Si_o$); i: Si in phytoliths; j: Si in crystalline silicate minerals ($Si_{tot}$ - $Si_d$)) in cultivated (in grey) and forest (in black) soils of the paired sites studied. Forest sites correspond to composite values (0-25 cm) calculated considering the thickness of the two sampled horizons (0-5 cm and 5-25 cm), their concentrations in the different elements and their respective bulk densities. Error bars correspond to the analytical uncertainties.

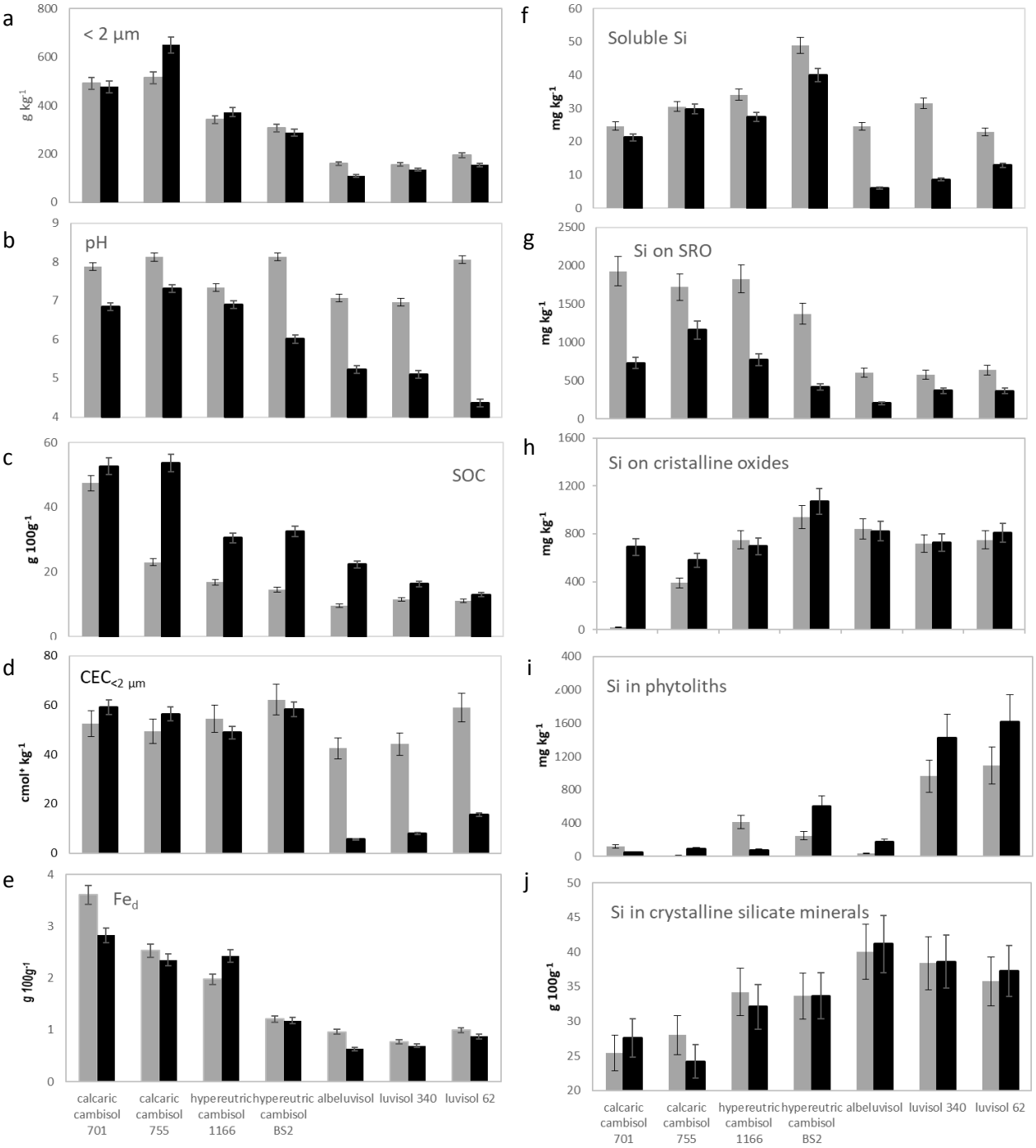

**Fig 3**: Relative abundance of (a) grass phytoliths (including RONDEL, CRENATE, BILOBATE, POLYLOBATE, and CROSS silica short cells, silicified epidermal tissues, FLABELLATE BULLIFORM cells, and ELONGATE DENDRITIC), (b) forest indicator phytoliths (including SPHEROIDS, sclereids and other silica bodies observed in woody dicotyledons, two BLOCKY faceted bodies typical of conifers, and a very long and large ELONGATE phytolith typical of some ferns (see details in SI Table-Phyto). (c) Relative abundance of ELONGATE DENDRITIC phytoliths typical of grass inflorescences. Bars represent 95% confidence intervals. Percentages were calculated based on (a, b) total sum of particles counted and (c) on total phytolith sum.

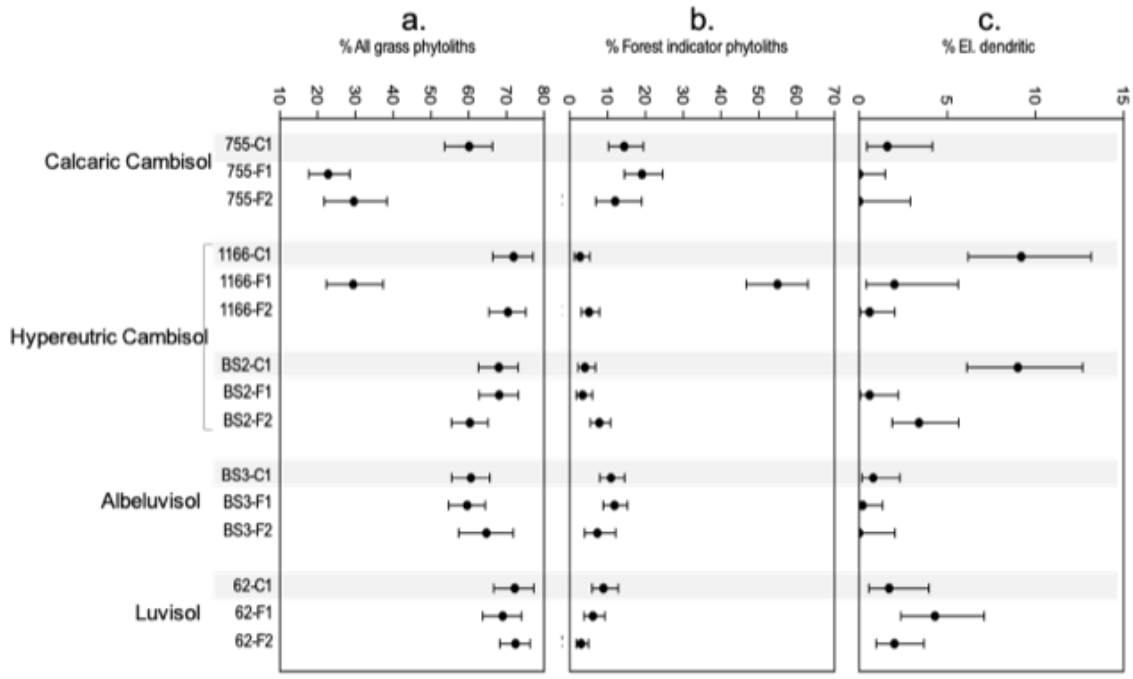

Fig. 4: XRD patterns of the < 2 µm fraction on oriented slides of the cultivated (in grey) and forest (in orange) soils: a- for the calcaric Cambisol 701; b- the Hypereutric Cambisol 1166; c- the Luvisol 340; and d- the Albeluvisol.

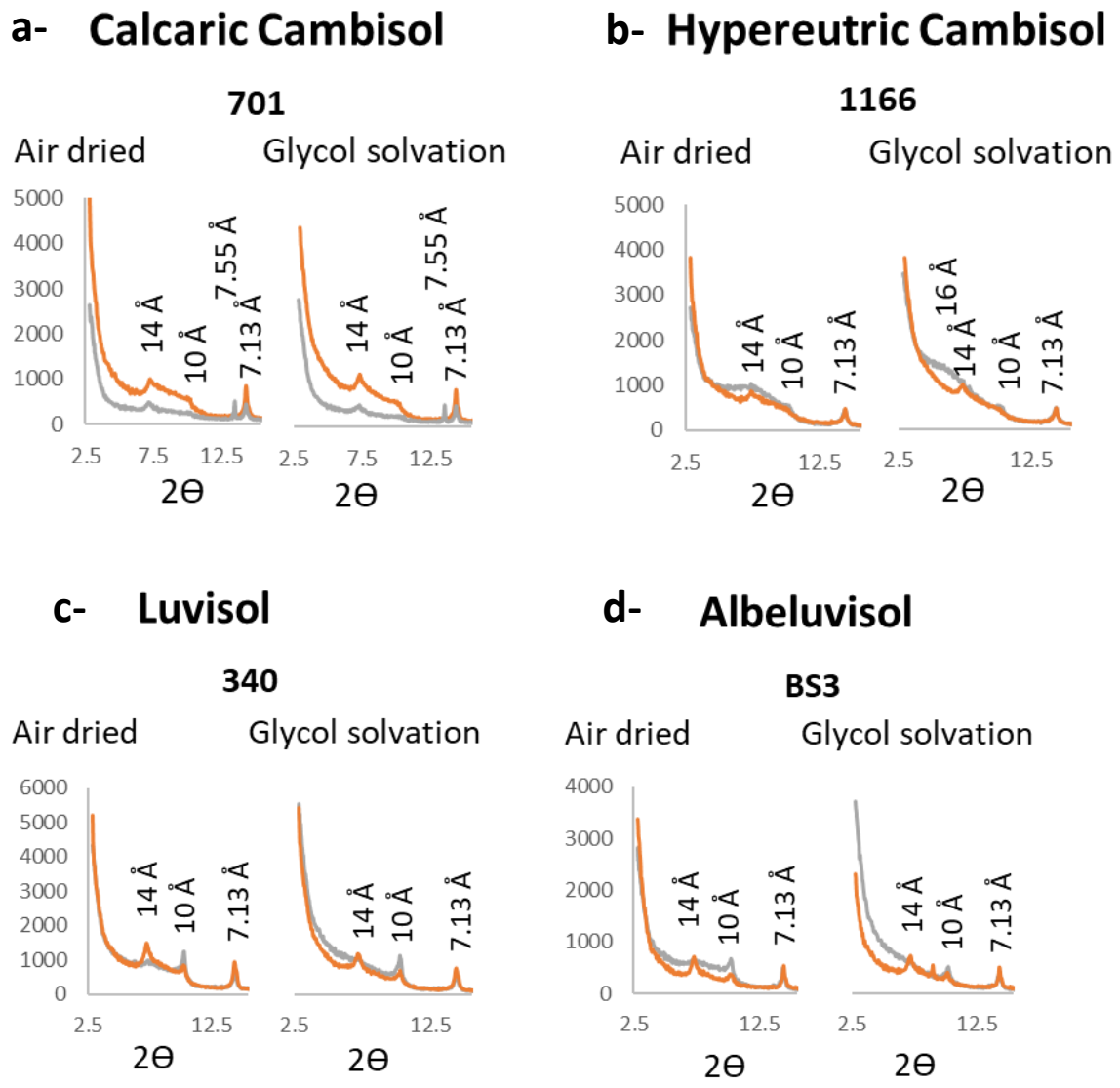

Figure 5: TEM image of a few discrete spherical particles interpreted as allophane (Kitagawa, 1971; Henmi and Wada, 1976; Parfitt, 1990) at the edges of clay particles (see in the circles) for the cultivated BS3 site. Spherical particles have diameter of 6 nm and are composed of a disc with a white central part interpreted as being the projection of a hollow sphere. It was not possible to observe them individually and they are systematically associated with clay particles.

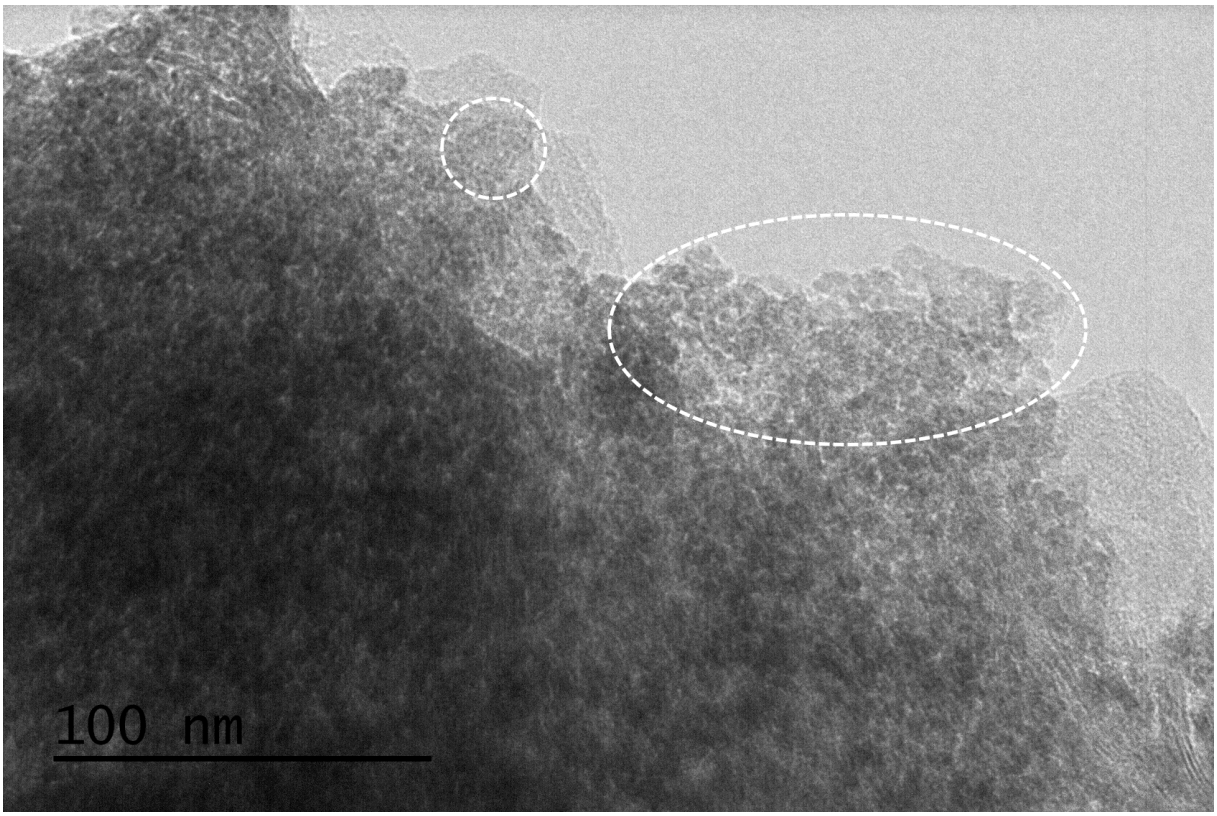

Figure 6: Impact of land use on the allophane amount in the paired sites: a- $Al_o$ as a function of $Si_o$; b- amount of allophane as a function of the < 2 µm concentration. Allophane content was calculated using Harsh's (2005) equation: % allophane = $Si_o/(-0.067\ Al_o/Si_o + 0.27)$. Forest soils are reported as black squares and the cultivated soils as grey circles. Pearson correlation coefficient and p-values provided on the figures were calculated excluding the samples identified by their name (for figure a only). Forest sites correspond to composite values (0-25 cm) calculated considering the thickness of the two sampled horizons (0-5 cm and 5-25 cm), their concentrations in the different elements and their respective bulk densities.

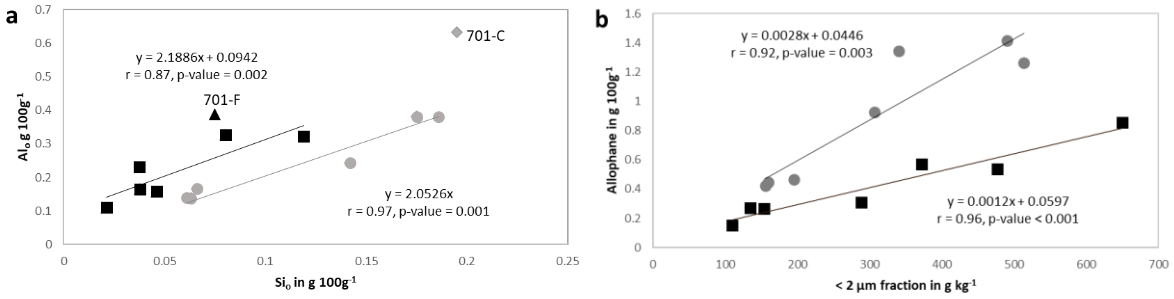

Figure 7: Soluble Si ($Si_{CaCl2}$) as a function of the allophane amount (a) and pH (b) in forested soils in black squares and cultivated soils in grey circles. Allophane content was calculated using Harsh's (2005) equation: % allophane = $Si_o/(-0.067\ Al_o/Si_o + 0.27)$. The grey rectangle corresponds both to the point of zero charge of the allophane and to the equilibrium with calcite. In both cases, the regression line was performed on all the soils that are not identified. Forested sites correspond to composite values (0-25 cm) calculated considering the thickness of the two sampled horizons (0-5 cm and 5-25 cm), their concentrations in the different elements and their respective bulk densities.

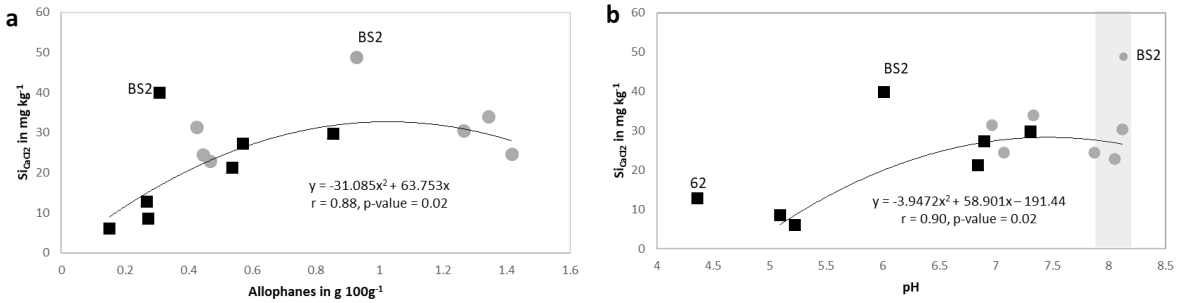

Figure 8: Adaptation of the Struyf et al. (2010) conceptual model for the impact of land use change from mature forests to long-term cultivated areas on the main pools that control soluble Si in soils developed on loess (left-hand side) and calcaric soils (right-hand side). Boxes represent the main Si pools with the size of the boxes representing the relative size of the stock. Arrows represent fluxes with a thickness depending on their relative importance. Dashed arrows represent irrelevant fluxes. Ph, Si in phytoliths; DSi, soluble Si estimated by $Si_{CaCl2}$; Allo, Si in allophane

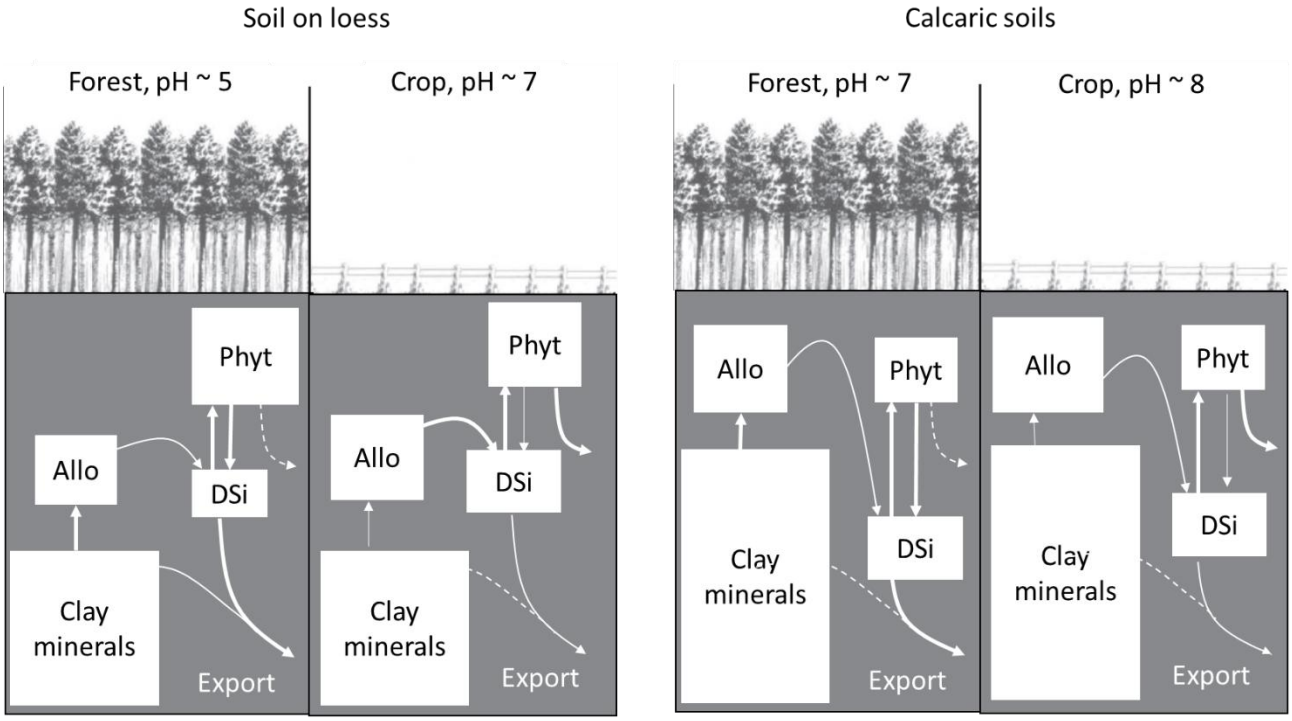

## Tables

Table 1: The Si pools: $Si_{tot}$, smooth Si extracted concentrations ($Si_o$, $Si_d$ and $Si_{CaCl2}$) and phytolith weight corrected from counting (see text); Si phyt equals phytoliths x 0.42 (see text). (*) The percentage of corroded phytoliths was evaluated on elongated and blocky morphotypes using the microscopic characteristics presented in figure SI2.

| **Soil** | **Land use** | **Vegetation/ crop rotation** | **Sample** | **$Si_{tot}$** | **$Si_o$** | **$Si_d$** | **$Si_{CaCl2}$** | **Phytoliths** | **Corroded phytoliths** |
|---|---|---|---|---|---|---|---|---|---|
| | | | | --------g $100g^{-1}$ ------- | | | mg $kg^{-1}$ | g $100g^{-1}$ | %(*) |
| Calcaric Cambisol | Agric. | N.D. | 701C1 | 26 | 0.19 | 0.20 | 24.6 ± 0.1 | 0.030 | nd |
| | Forest | Beech and other deciduous trees | 701F1 | 28 | 0.075 | 0.14 | 21.2 ± 0.5 | 0.011 | nd |
| | Agric. | N.D. | 755C1 | 28 | 0.17 | 0.21 | 30 ± 2 | 0.002 | nd |
| | Forest | N.D. | 755F1 | 24 | 0.12 | 0.19 | 35 ± 5 | 0.028 | nd |
| | | | 755F2 | 25 | 0.12 | 0.17 | 25.2 ± 0.3 | 0.021 | nd |
| Hypereutric Cambisol | Agric. | Cereals | 1166C1 | 34 | 0.19 | 0.26 | 34 ± 1 | 0.102 | 33 ± 1 |
| | Forest | Maple, hornbeam, oak | 1166F1 | 31 | 0.072 | 0.14 | 37 ± 1 | 0.006 | 60 ± 3 |
| | | | 1166F2 | 32 | 0.083 | 0.15 | 24 ± 1 | 0.023 | nd |
| | Agric. | Wheat/barley | BS2C1 | 34 | 0.14 | 0.24 | 48.8 ± 0.4 | 0.064 | 62 ± 6 |
| | Forest | Pine, various deciduous trees | BS2F1 | 33 | 0.046 | 0.16 | 40 ± 3 | 0.091 | 32 ± 2 |
| | | | BS2F2 | 34 | 0.046 | 0.14 | 39.6 ± 0.3 | 0.239 | 50 ± 2 |
| Luvisol | Agric. | Cereals | 340C1 | 39 | 0.061 | 0.13 | 31.4 ± 0.7 | 0.246 | nd |
| | Forest | Deciduous trees | 340F1 | 37 | 0.028 | 0.1 | 7.2 ± 0.9 | 0.066 | nd |
| | | | 340F2 | 40 | 0.046 | 0.12 | 9.6 ±0.5 | 0.616 | nd |
| | Agric. | N.D. | 62C1 | 36 | 0.066 | 0.14 | 22.8 ±0.3 | 0.292 | 25 ± 1 |
| | Forest | Conifer | 62F1 | 36 | 0.031 | 0.14 | 9.3 ± 0.3 | 0.646 | 37 ± 1 |
| | | | 62F2 | 38 | 0.039 | 0.11 | 14 ± 2 | 0.351 | 52 ± 8 |
| Albeluvisol | Agric. | Wheat, maize, rape | BS3C1 | 40 | 0.063 | 0.147 | 24.5 ± 0.3 | 0.009 | 36 ± 6 |
| | Forest | Oak, holly, hazel tree | BS3F1 | 41 | 0.018 | 0.099 | 5.9 ± 0.4 | 0.046 | 44 ± 3 |
| | | | BS3F2 | 42 | 0.037 | 0.125 | 6.9 ± 0.3 | 0.029 | 56 ± 6 |

Table 2: Pearson correlation coefficients (r) and associated p-values of $Si_{CaCl2}$ with the main soil variables analysed for the 21 samples of the seven soil pairs (2 samples per forest and one per crop plot). Coefficients in bold are significant at a 5 % level of confidence.

| Variables | < 2 µm | 2-20 µm | 20-50 µm | 50-200 µm | 200-2000 µm | SOC | pH |
|---|---|---|---|---|---|---|---|
| r | **0.493** | -0.424 | -0.410 | -0.297 | 0.105 | 0.267 | **0.614** |
| p-values | **0.023** | 0.055 | 0.065 | 0.192 | 0.651 | 0.241 | **0.003** |

| Variables | $Si_o$ | $Al_o$ | $Fe_o$ | $Si_d$ | $Al_d$ | $Fe_d$ | $Si_{tot}$ | $Al_{tot}$ | $Fe_{tot}$ |
|---|---|---|---|---|---|---|---|---|---|
| r | **0.526** | 0.261 | -0.186 | **0.684** | 0.261 | 0.373 | **-0.479** | **0.452** | **0.483** |
| p-values | **0.014** | 0.253 | 0.420 | **0.001** | 0.254 | 0.096 | **0.028** | **0.039** | **0.026** |

| Variables | phytoliths | CEC | $CEC_{<2µm}$ |
|---|---|---|---|
| r | -0.360 | **0.602** | **0.824** |
| p-values | 0.109 | **0.004** | **<0.0001** |